Composites: Part A 190 (2025) 108595

Contents lists available at ScienceDirect

Composites Part A

journal homepage: www.elsevier.com/locate/compositesa

Adjustable-stiffness and programmable shape memory polystyrene composites with elastic fibers for complex structure smart molds

Xiaoyu Du [a], Fenghua Zhang [a], Likai Hu [a], Lan Luo [a], Zhengxian Liu [a], Yanju Liu [b], Jinsong Leng [a,*]

[a] Centre for Composite Materials and Structures, Harbin Institute of Technology (HIT), No.2 Yikuang Street, Harbin 150000, PR China
[b] Department of Astronautic Science and Mechanics, Harbin Institute of Technology (HIT), No. 92 West Dazhi Street, Harbin 150000, PR China

ARTICLE INFO

Keywords:
A. Smart materials
A. Thermosetting resin
A. Polymer-matrix composites (PMCs)

ABSTRACT

Smart molds based on shape memory polymers (SMPs) with active deformation characteristics enable demolding of complex structures in response to external stimuli. However, for large-cavity components, smart molds made of common SMPs often have problems such as limited deformation and being prone to blowing during molding. Based on free radical polymerization, a rigid-flexible cross-linked network structure was constructed, achieving a large deformation up to 370 % for thermosetting shape memory styrene. On this basis, composites with nylon-spandex elastic fiber was prepared. The introduction of ± 45° laid elastic fibers hinders the crack propagation in the matrix and can improve the deformation capacity of the composites. Further, the programmable composites were applied to reusable shape memory smart molds, accomplishing shape convertion from 2D planes to 3D structures and 3D mandrels to 4D deformable components with variable cross-sections, curvatures, and structures, which is expected to pave a new way for smart molds.

1. Introduction

In the manufacturing industry, mold is a crucial tool for component forming, with an irreplaceable position [1,2]. With the technological development in manufacturing engineering, the design and production of complex components have higher requirements. The production of components with variable structure, variable curvature, variable cross-section and other characteristics is difficult to be achieved by the traditional manufacturing technology. At present, there are major problems such as difficult releasing, complicated design, and high mold self-weigh, severely limiting the development of complex components [3–5]. Therefore, developing new molds easy to release has become an urgent problem to be solved in the manufacturing industry.

Shape memory material is known to be a smart material that can actively recover its initial shape in response to a variety of external stimuli such as thermo [6–8], electric [9–12], light [13–15], magnet [16–18], pH [19,20] and so on. Due to the advantages of light weight, high strength, and diverse actuation modes, shape memory polymers (SMPs) have been widely used in aerospace [21–25], biomedical [26,27], and machinery manufacturing fields [28–30], with a wide range of potential applications [31,32]. Combining SMPs capable of active deformation characteristics with the molding of complex components and using SMPs to manufacture shape memory smart molds can effectively reduce the difficulty of releasing complex components and achieve automatic demolding, which is expected to solve the demolding problems [33].

Presently, SMP smart molds have been successfully applied to the manufacturing of filament-wound parts. It has been investigated that bottle-shaped and S-shaped filament-winding composite components can be fabricated and easy releasing can be achieved with the assistance of SMP smart molds [33–36]. Everhart et al. [36] first applied shape memory polystyrene to smart molds by fabricating bottle-shaped and S-shaped mandrels, and verified the feasibility of shape memory smart molds by filament winding process. Lei Zhang et al.[35] fabricated bottle shaped and irregular section styrene-based SMP smart molds with radial deformation rate of 25 %, and their shape recovery rate was close to 100 % when the temperature was higher than the glass transition temperature(T_g). Although existing SMP smart molds can contribute to the demolding, smart molds for large cavity components are prone to problems such as tearing and breakage during the molding process, restricting the application scope of smart molds. Therefore, there is an urgency to develop SMPs with large deformation capacity at

* Corresponding author.
E-mail address: lengjs@hit.edu.cn (J. Leng).

https://doi.org/10.1016/j.compositesa.2024.108595
Received 11 September 2024; Received in revised form 26 October 2024; Accepted 13 November 2024
Available online 26 November 2024

Table 1
SMPs in different ratios.

sample	BPO	ST	BA	cross-linking agent
SMP1	0.60 g	24.00 g	6 g	DVB 0.60 g
SMP2	0.60 g	24.00 g	6 g	PEGDA 200 0.92 g
SMP3	0.60 g	24.00 g	6 g	PEGDA 400 1.84 g

deformation temperature and at the same time has a certain strength at room temperature to broaden the development path of smart molds and assist the manufacturing upgrade of complex components.

In this work, the large deformation thermoset shape memory polystyrene was developed by the rigid-flexible coupling molecular network design, with maximum elongation at break more than 370 %, based on which the composites involved by nylon and spandex elastic fiber cloth were prepared. The programmable composites were applied to shape convertion from 2D planes to 3D structures and 3D mandrels to 4D deformable components which is expected to pave a new way for smart molds.

2. Experimental section

2.1. Materials

Styrene (ST), poly(ethylene glycol) diacrylate (PEGDA) with average molecular weight 200 and 400, benzoyl peroxide (BPO) were purchased from Shanghai McLean Biochemistry Technology Co. n-Butyl Acrylate (BA), Divinylbenzene (Divinylbenzene, DVB) were purchased from Shanghai Aladdin Biochemical Technology Co. Anhydrous ethanol was purchased from Tianjin Fine Chemical Co. The fiber mesh fabric was produced by Zhuji Ailong Knitting Co., Ltd, with 83.4 % nylon and 16.6 % spandex. All raw materials are used as is.

2.2. Synthesis of SMPs

SMPs were prepared by the simple one-pot method with proper contents of BPO as an initiator [37]. ST and BA are taken in a beaker according to the ratio shown in Table 1. The cross-linking agent DVB or PEGDA and initiator BPO are added. Stir for 20 min to make sure that the chemicals are fully mixed. The obtained premix was injected into the well-prepared mold and placed in an oven for curing according to the gradient process of 50 °C 2 h, 90 °C 2 h, and 120 °C 3 h. After cooling and demolding, the shape memory polystyrene samples SMP1, SMP2, and SMP3 were obtained respectively.

2.3. Synthesis of shape memory polymer composites (SMPCs)

Fig. 1(b) shows the fabrication of SMPCs. Fiber mesh cloth with a proper size was laid and fixed in the mold at preset angle, and the SMPC samples named SMPC1 and SMPC2 respectively can be manufactured according to the process of 2.2 and Table 2.

3. Results and discussion

3.1. Properties of the SMPs

The synthesis process of SMPs is shown in Fig. 1(a). Simple and controllable one-pot synthesis method is applied to achieve free radical polymerisation by the thermal initiator, and the flexibility of segments of SMPs is varied by changing raw materials to construct a rigid-flexible

Table 2
SMPCs with different parameters.

sample	BPO	ST	BA	PEGDA 200	Laying angle
SMPC1	0.60 g	24.00 g	6 g	0.92 g	±45°
SMPC2	0.60 g	24.00 g	6 g	0.92 g	0°/90°

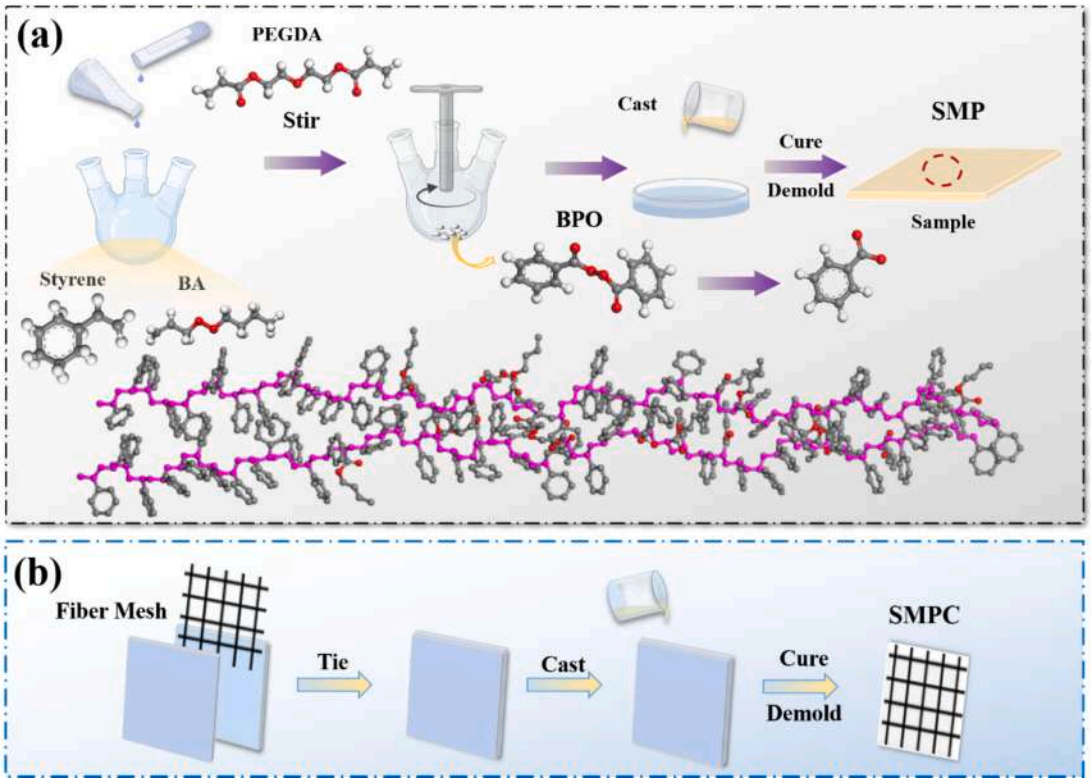

Fig. 1. (a) Synthesis and molecular structure schematic of SMPs; (b) Fabrication process of SMPCs.

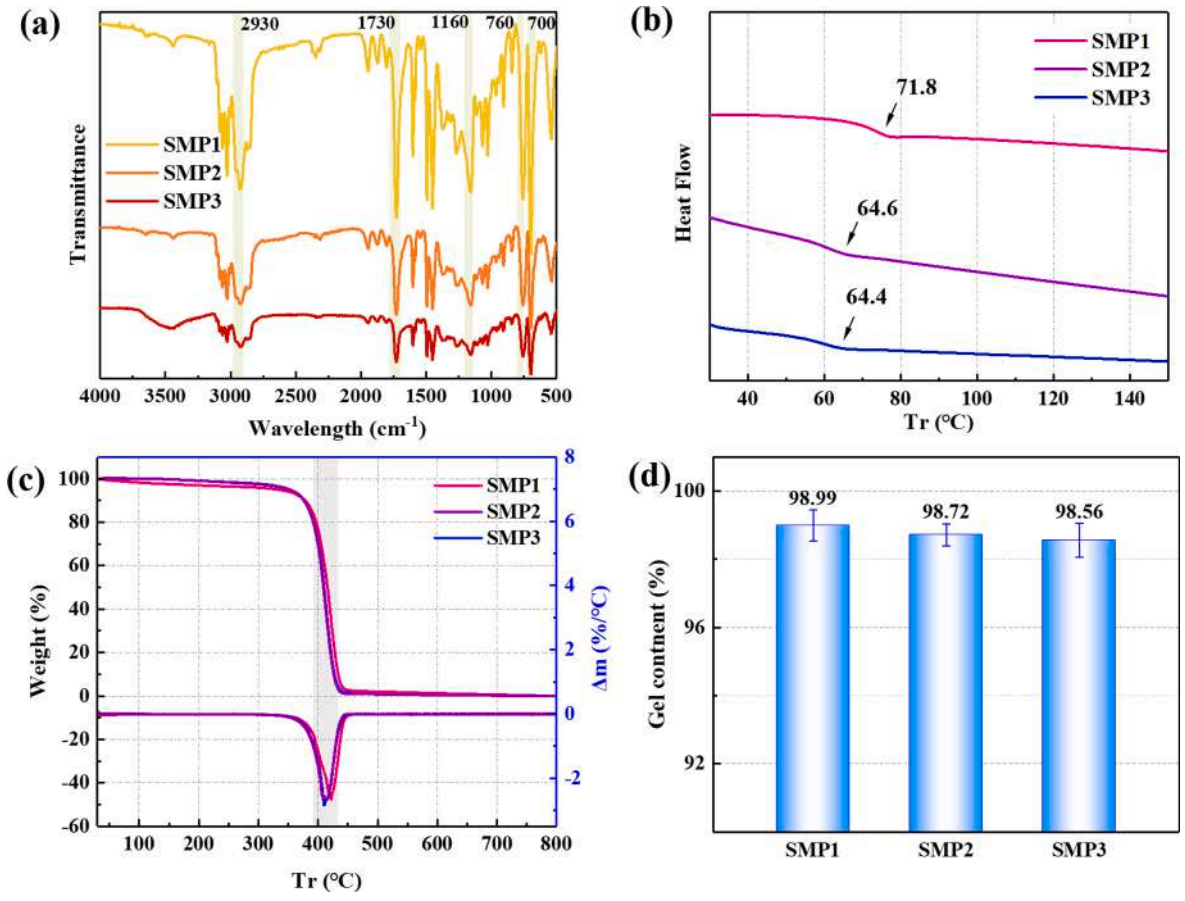

Fig. 2. (a) FTIR curves of SMPs; (b) DSC curves of SMPs; (c) TGA and DTG curves of SMPs; (d) Gel content of SMPs.

coupling polymer molecular network.

The characteristic functional groups of SMPs samples can be confirmed by FTIR, as shown in Fig. 2(a). Test details were provided in Supporting Information. The wave number corresponding to the carbon–carbon double bond (C═C) is usually at 1600 cm^{-1}-1670 cm^{-1}, with no peaks, suggesting that the C═C in the monomer has been involved in the reaction. There are the mono-substituted peak of the benzene ring at 700 cm^{-1} and 760 cm^{-1} and the absorption peak of the carbonyl group at 1730 cm^{-1}, showing the formation of the polymer three-dimensional cross-linking network.

DSC measures T_g by observing thermodynamic behaviors such as heat absorption and release during the heating process of samples, and can also reflect the crystalline changes, phase changes such as melting and solidification, as well as the heat absorption and release of chemical reactions in materials. Fig. 2(b) shows the DSC curve of SMP samples. There is no heat absorption peak of crystal melting, confirming that the SMPs are amorphous polymers. The curve indicates that the T_g of the SMPs are 71.8 °C, 64.6 °C and 64.4 °C, respectively, exhibiting a decline. As the flexibility of the cross-linking agent increases, there are more flexible chain segments in the polymer network travelling at lower temperatures, which is macroscopically manifested by a decreasing trend in the T_g of the samples.

TGA with N_2 atmosphere was carried out to investigate the thermal stability properties of SMPs. As shown in Fig. 2(c), the thermal degradation of SMPs mainly went through two stages. In the first stage, the mass loss of SMPs is not significant, which mainly caused by the volatilisation of low-boiling-point substances. In the second stage, between 200 °C and 500 °C, there is a sharp mass loss suggesting fracture and decomposition of the polymer network due to the high temperature. The inflection point temperature (T_l) indicates the temperature at which the polymer mass loss is the fastest, namely, the temperature corresponding to the peak value of the DTG curve, which has been labelled. The main chains of the polymer networks of the three samples are all composed of C—C with similar pyrolysis temperatures, suggesting no obvious difference in the thermal stability performance.

Determination of the gel content of thermosetting polymers is a direct method of evaluating the curing reaction process, and Soxhlet extraction was used to test the gel content of samples with anhydrous ethanol as solvent. As shown in Fig. 2(c), the gel contents of SMP1, SMP2 and SMP3 after refluxing were 98.99 %, 98.72 % and 98.56 %, respectively, showing an increasing trend as the crosslinking density decreased, which was in accordance with the expectation.

3.2. Dynamic mechanical properties of SMPs and SMPCs

DMA measures the changes in mechanical properties such as storage modulus and loss factor of the SMPs with increasing temperature to obtain the T_g of the material. With the help of DMA, the mechanical properties of materials at different temperatures can be obtained, which can provide guidance for the shaping and application of SMPs. As shown in Fig. 3(a), the storage modulus of SMPs all show three stages. When the temperature is low, the material is in the glassy state with high storage modulus of 1.7–2.0 GPa. The rubbery state of the SMPs corresponds to the high temperature with a low modulus. As the temperature increases, the polymer molecules absorb more energy and allow internal molecular chain movement, manifested macroscopically as changing stiffness with temperature. The loss factor, Tan Delta, shows that the T_g of the SMPs, decreasing with the increase of the flexible chain segments and the mobility of the polymer network, which is the same trend as that reflected by DSC.

The DMA curve of SMPC1 is shown in Fig. 3(b), and the energy storage modulus image of SMPC1 is similar to that of SMPs, which are in

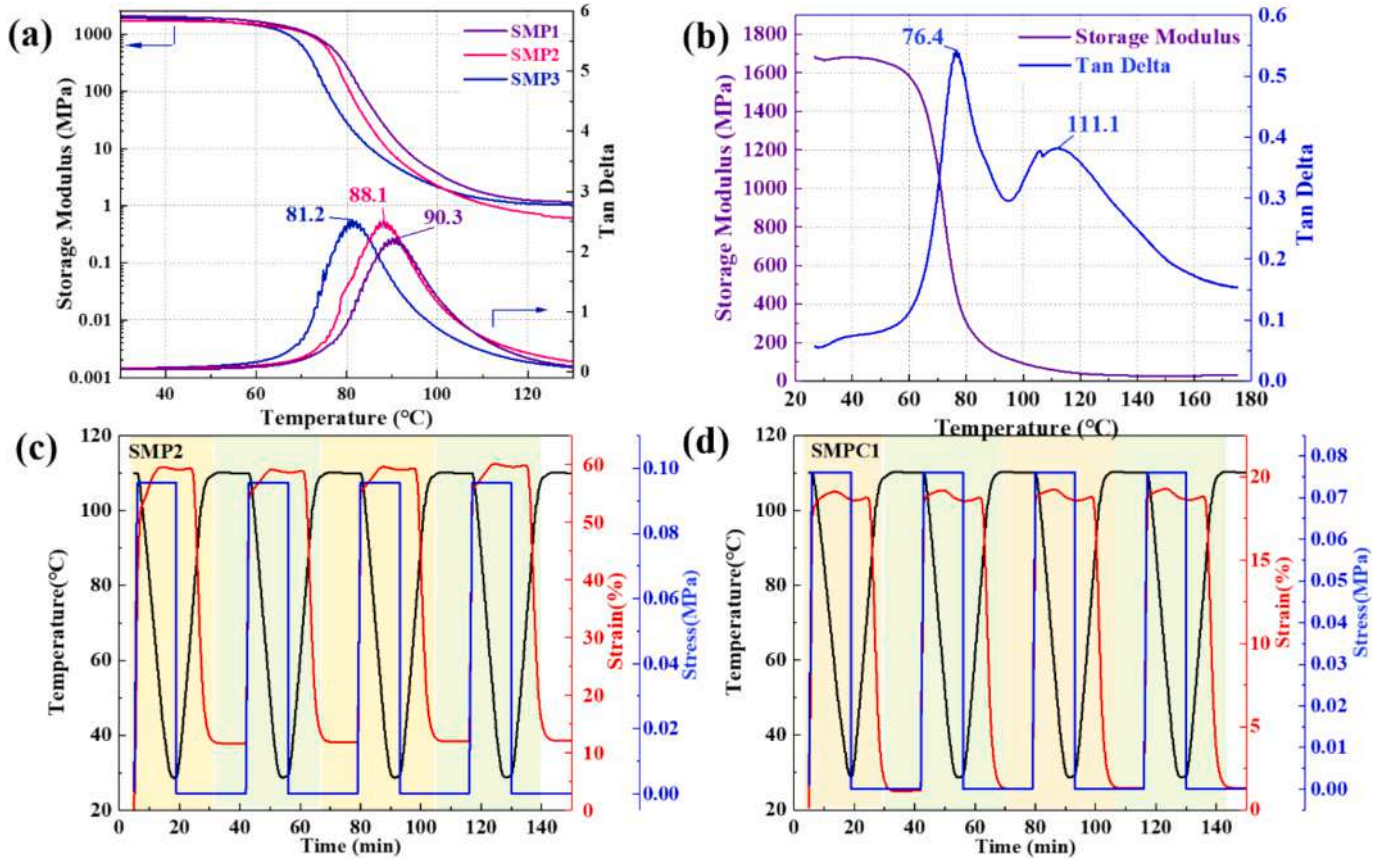

Fig. 3. (a) DMA curves of SMPs; (b) DMA curves of SMPC1; (c) Shape memory cyclic curves of SMP2; (d) Shape memory cyclic curves of SMPC1.

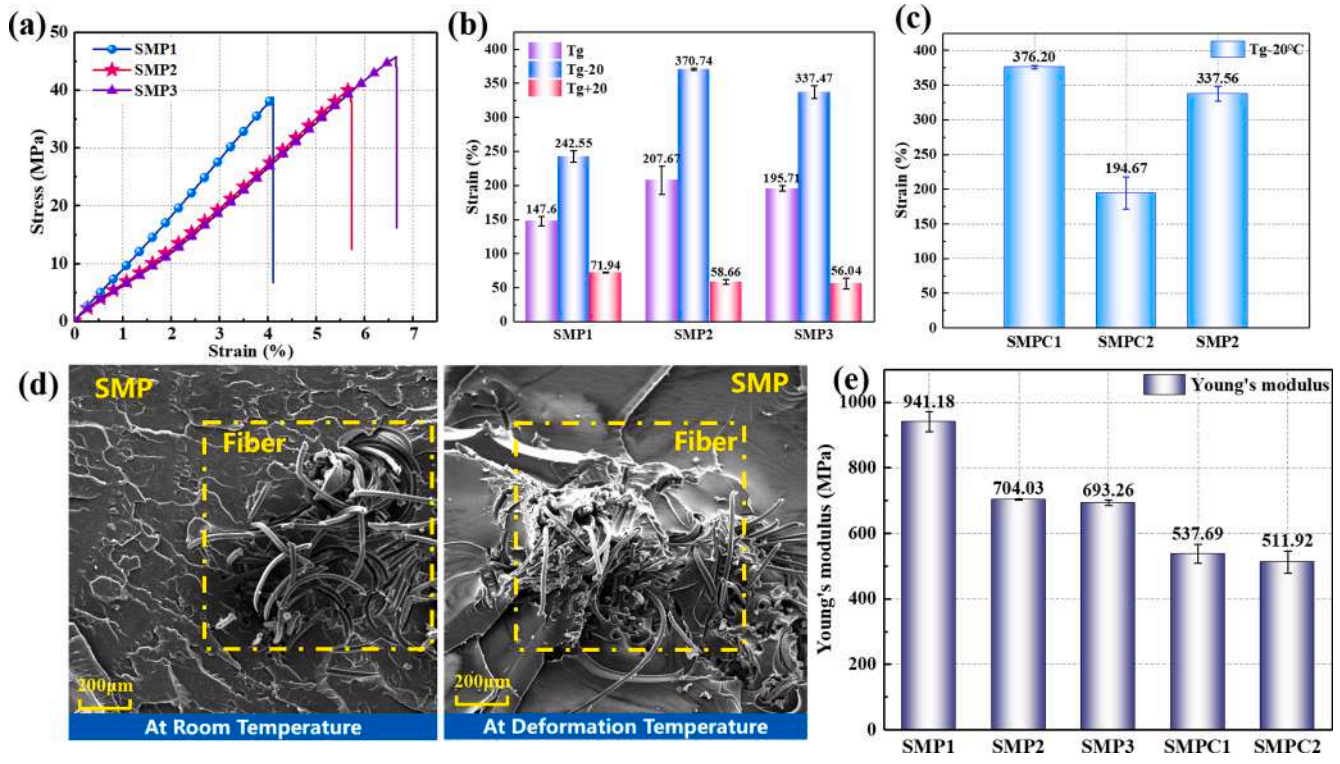

Fig. 4. (a) Room temperature tensile curves of SMPs; (b) Elongation at break of SMPs at different temperatures; (c) Elongation at break of SMPCs and SMP2 at T_g-20 °C; (d) SEM images of fracture cross sections of SMPC1 at room temperature and T_g-20 °C; (e) Histograms of Young's modulus at room temperature of SMPs and SMPCs.

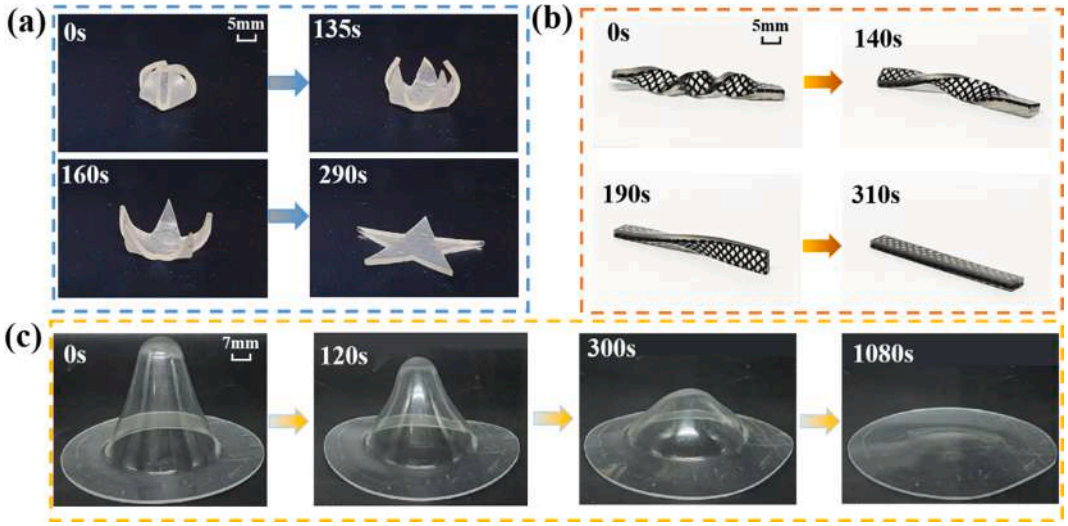

Fig. 5. Shape memory recovery process at 85 °C of (a) SMP1, (b) SMPC1, (c) SMP2.

three stages. Due to the introduction of the second phase, there are two peaks in the loss factor curves, corresponding to temperatures of 76.4 °C and 111.1 °C, respectively. Since the fiber mesh and the resin matrix in SMPCs are two phases having their own transition temperatures that interact with each other but are independent of each other, the overall loss factor of SMPC shows two peaks. Elastic fibers are soft and flexible at both room temperature and deformation temperature, making it difficult to store energy without load; SMP matrix has a certain strength at room temperature, and is elastically deformable at deformation temperature. It can absorb and store energy during the molding process, and release energy to drive SMPCs recovery. As shown in Fig. S4, at the same recovery temperature and with similar deformation degree, the higher the SMP content, the greater the driving energy per unit of SMPC, and the faster the shape memory recovery speed. Therefore, the deformation ability and shape memory effect are more limited by the resin matrix, so the samples are able to show deformation ability near the first peak, which is near the T_g shown by the matrix. The four-cycle shape memory cycling curves of SMP2 and SMPC1 are shown in Fig. 3(c) and (d), respectively. Based on the changes in strain, the material's fixation rate and recovery rate can be calculated. After four cycles, the shape fixation rate and shape recovery rate of SMP2 and SMPC1 can reach more than 99 %, suggesting excellent shape memory performance.

3.3. Mechanical properties of SMPs and SMPCs

The static tensile curves of SMPs at room temperature are shown in Fig. 4(a). With the of cross-linking agents' flexibility, mobility of the polymer network increases, leading to a growth in the elongation at break of SMPs. Meanwhile, the introduction of flexible segments in PEGDA caused a significant decrease in the elastic modulus. While the lengths of the chain segments of PEGDA 200 and PEGDA 400 did not have a significant effect on the modulus, which may be due to the fact that they are both more flexible cross-linkers compared to DVB with relative polymerization degree, making the difference in the elastic modulus tiny. Fig. 4(e) shows the elastic modulus of SMPs and SMPCs at room temperature. Compared to the matrix, the incorporation of the fiber mesh reduces the strength of the composites but enhances the ultimate strain at room temperature (Fig. S2).

The static tensile elongation at break of SMPs measured at different temperatures with a scale segment of 40 mm is shown in Fig. 4(b). The elongation at break of SMPs decreases with increasing temperature in all the three selected temperatures, which is due to the fact that a certain degree of high temperatures weakens the intermolecular forces of the polymer and reduces the strength and stability of the bonds. At T_g-20 °C, the introduction of PEGDA significantly increases the elongation at break of the samples, and SMP2 shows the highest elongation at break of up to 370 %, which is 120 % higher compared to SMP1. This is due to the long-chain cross-linking agents making the cross-linking density of the polymer network lower and the movable distance of the molecular chain segments rising, which was macroscopically manifested in the increase of elongation at break. The static tensile elongation at break of SMPCs and SMP2 at T_g-20 °C is given in Fig. 4(c), with a 10 mm scale segment. The ± 45°-layered fiber mesh positively affects the elongation at break of the material, whereas 0°/90°-layered fiber mesh has a negative effect. The ± 45°-layered fiber mesh is able to share the load during tension and the mesh structure can inhibit crack extension at the same time, improving the tensile performance of SMPC1. While the 0°/90°-layered fiber mesh can share the load, but the 90°-layered fiber are more prone to splitting under tension, which promotes the fracture. The SEM image of the cross-section of SMPCs at T_g −20 °C confirms this point (Fig. S3).

From Fig. 4(d), it can be seen that the matrix is able to impregnate the fiber filaments and the two have good bonding. At room temperature and T_g-20 °C, the fracture cross sections of the tensile parts show synchronous fracture of the fibers and the matrix with no fiber pulling out, showing that the fibers and the matrix have a good form-following property.

3.4. Shape memory behavior

SMPs and SMPCs are shaped at 110 °C and then cooled to room temperature to fix their temporary structure. The shape memory performance of samples in temporary shapes were tested at 85 °C, and the recovery process is shown in Fig. 5. Fig. 5(a) shows the process of SMP1 from a temporary closed flower bud gradually unfolding into a permanent pentagonal star. Under thermal simulation, the sample can basically complete recovery within 290 s. The SMPC1 was twisted into a spiral component when in high elastic state. As shown in Fig. 5 (b), the component overcomes the friction between the specimen and the environment with the assistance of shape recovery driving force, achieving autonomous recovery within 310 s successfully. The SMP2 3D taper shown in Fig. 5 (c) is manufactured from a 2D sheet, which is able to achieve large deformation recovery within 1026 s of high temperature response. The recovery process is shown in video S1.

3.5. Shape memory smart structures and applications

SMPs and SMPCs have the properties of high modulus at room temperature and large deformation at deformation temperature (Fig. 6

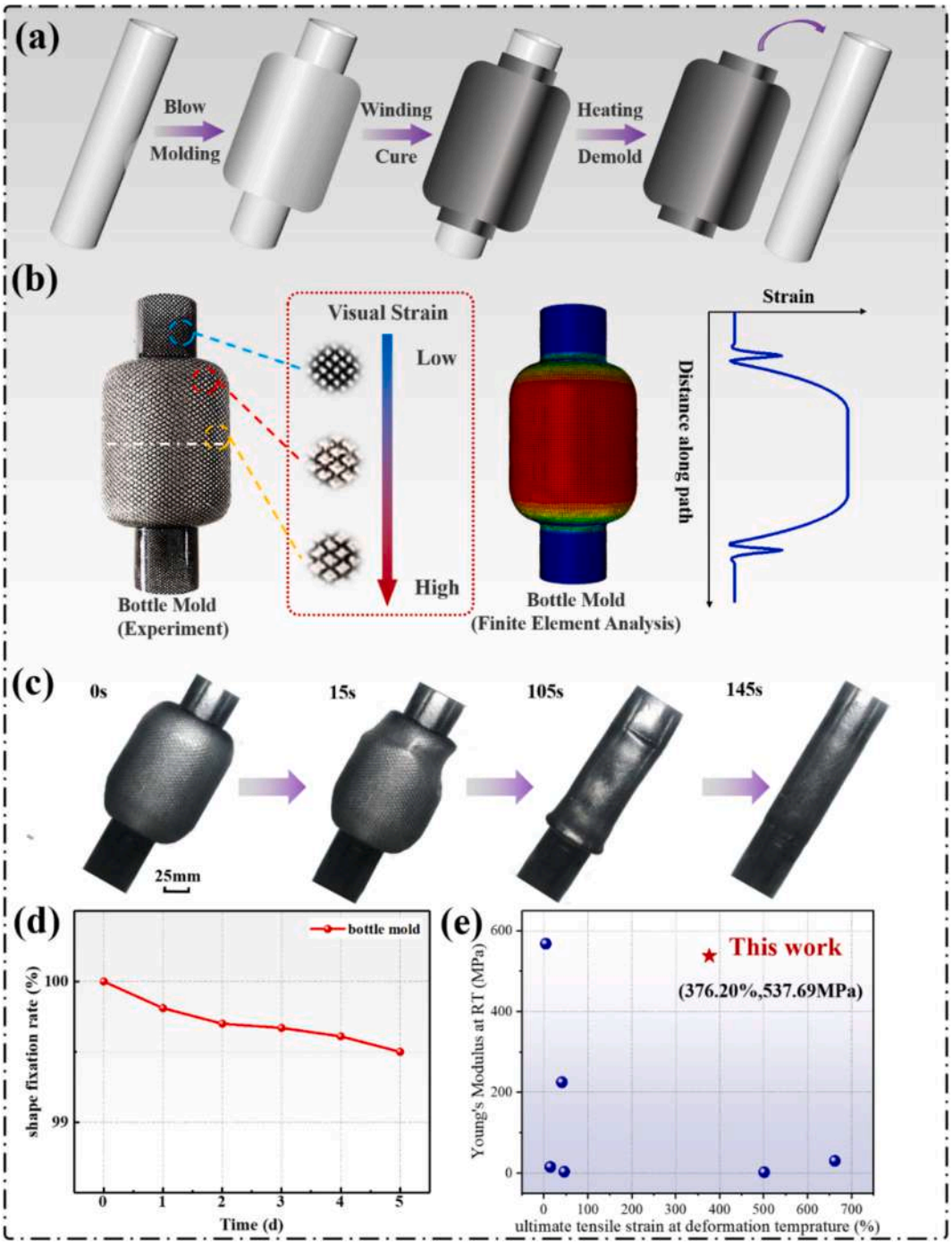

Fig. 6. (a) Schematic diagram of the working process of the bottle smart mold; (b) Experiment and finite element analysis of the bottle mold; (c) Response process of the bottle smart mold at 110 °C; (d) Shape fixation rate of the bottle smart mold at 5d after blowing; (e) Comparison of the performance with the other shape memory polystyrenes[38–43].

(e)), enabling them more advantageous for applications in smart molds and other fields compared with other shape memory polystyrene [38–43].

Fig. 6(a) shows the working process of the shape memory smart mold. After the filament winding on its surface and curing, the composite component is shaped. Then the temperature is raised to above T_g, the smart mold actively deforms and returns to the initial shape, achieving the rapid demolding of large cavity components. For the bottle mold with 100 % deformation, ABAQUS software is used to simulate the blowing process, with 2 mm initial thickness of the mandrel and 1 MPa blowing air pressure. The output stress map is shown in Fig. S1. In the process of molding, the mid-portion of the smart mold has the largest deformation, and it is also the region with larger stress. The location of the maximum stress appears in the stress concentration region at the corner. The experiment and finite element analysis results of the bottle mold are shown in Fig. 6(b), and the right curve shows the strain magnitude of the mold output along the axial direction. Combined with figure of the experiment bottle mold, it can be seen that the addition of the elastic fiber mesh enables the local deformation degree of the mold to be displayed by the degree of mesh distortion, which results in the intuitive visualization of the degree of deformation. Fig. 6(c) shows the quick recovery process of the bottle mold at 110 °C within 145 s, and

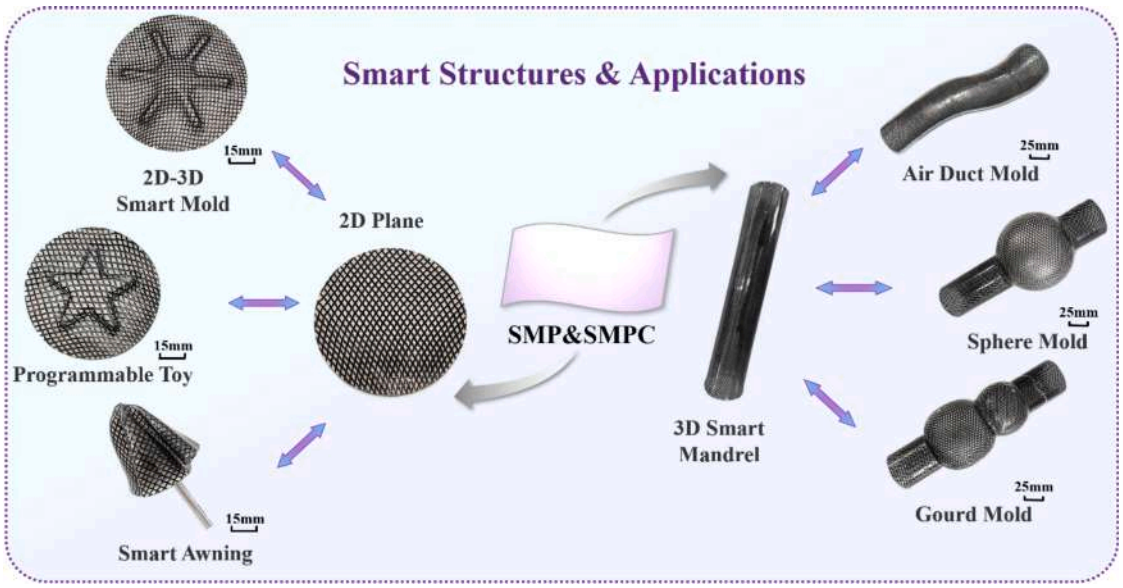

Fig. 7. SMPs and SMPCs' smart structures and applications.

more details are displayed in Video S2. The smart molds can maintain their shapes within 5 days after blowing, with shape fixation rate more than 99 % (Fig. 6(d)), satisfying the basic needs of the smart molds for shaping, transportation and usage. Compared with other shape memory polystyrenes (Fig. 6(e)), the SMPs designed and prepared in this work have the advantages of high modulus at room temperature and large deformation at deformation temperature, which are expected to promote the technological upgrading of smart molds for the production of large cavity components.

As shown in Fig. 7, at the deformation temperature, composite materials with reconfigurable properties can be transformed from 2D planes to 3D structures by external forces, achieving multi-domain and multi-purpose applications of 2D-3D smart molds, programmable toys, and smart awnings. The 3D composite mandrel is formed into 4D deformable large cavity component with variable cross-section, curvature, and structures. According to different usage scenarios, it realizes the development of smart molds with multiple forms and uses such as air duct molds, sphere molds and gourd molds, broadening the new path for the application of smart molds.

4. Conclusion

In this work, thermosetting shape memory styrene with high modulus at room temperature and large deformation characteristics at deformation temperature through rigid-flexible coupling molecular design were synthesized, ultimate strain of which can reach 370 %. Furthermore, composites were developed with spandex-nylon blended elastic fiber introduced, which can suppress the propagation of cracks and enhance the deformation ability of the composite. The shape recovery rate and shape fixation rate of the produced SMP and SMPC are both above 99 %, demonstrating excellent shape memory performance. Based on the large deformation and reconfigurability properties, SMPCs was demonstrated in the fields of 2D-3D smart molds, programmable toys, and smart awnings by 2D sheets to 3D shape convertion. 4D deformable smart molds with variable cross-section, curvature and structure have been achieved from 3D mandrels for active demolding, demonstrating the superiority of fast and convenient molding in complex components. Thermosetting shape memory styrene and composites are expected to promote the efficient preparation of complex cavity structure composite components, paving a new way to advanced manufacturing.

CRediT authorship contribution statement

Xiaoyu Du: Writing – original draft, Methodology. **Fenghua Zhang:** Writing – review & editing, Project administration, Funding acquisition. **Likai Hu:** Investigation, Data curation. **Lan Luo:** Methodology, Investigation, Data curation. **Zhengxian Liu:** Investigation, Data curation. **Yanju Liu:** Supervision, Resources. **Jinsong Leng:** Supervision, Resources, Funding acquisition.

Declaration of competing interest

The authors declare that they have no known competing financial interests or personal relationships that could have appeared to influence the work reported in this paper.

Acknowledgments

We thank the National Natural Science Foundation of China (Grant No. 92271112) for the support of this work.

Appendix A. Supplementary data

Supplementary data to this article can be found online at https://doi.org/10.1016/j.compositesa.2024.108595.

Data availability

Data will be made available on request.

References

[1] Altan T, Lilly B, Yen YC. Manufacturing of dies and molds. Cirp Annals-Manufacturing Technol 2001;50(2):405–23.
[2] Chen CR, Wang Y, Ou HG, He Y, Tang XZ. A review on remanufacture of dies and moulds. J Clean Prod 2014;64:13–23.
[3] Kuo CC, Qiu SX, Lee GY, Zhou J, He HQ. Characterizations of polymer injection molding tools with conformal cooling channels fabricated by direct and indirect rapid tooling technologies. Int J Adv Manuf Technol 2021;117(1–2):343–60.
[4] Zadeh HN, Huber T, Nock V, Fee C, Clucas D. Complex geometry cellulose hydrogels using a direct casting method. Bioengineering-Basel 2020;7(2).
[5] Wang Y, Yu RL, Yin SK, Tan R, Lou YC. Effect of gel time of 3D sand printing binder system on quality of sand mold/core. China Foundry 2021;18(6):581–6.
[6] Winhard BF, Haida P, Plunkett A, Katz J, Domenech B, Abetz V, et al. 4D-printing of smart, nacre-inspired, organic-ceramic composites. Addit Manuf 2023;77.

[7] Tang ZZ, Gong JH, Cao PR, Tao LM, Pei XQ, Wang TM, et al. 3D printing of a versatile applicability shape memory polymer with high strength and high transition temperature. Chem Eng J 2022;431.
[8] Zhang C, Liu R, Tao C, Zhang C, Ji H, Qiu J. Design, construction, and modeling of aircraft door sealing plate based on SMAs. Int J Smart and Nano Materials 2022;13(3):481–503.
[9] Booth RE, Khanna C, Schrickx HM, Siddika S, Al Shafe A, O'Connor BT. Electrothermally actuated semitransparent shape memory polymer composite with application as a wearable touch sensor. ACS Appl Mater Interfaces 2022;14(47):53129–38.
[10] Umair MM, Zhang Y, Zhang SF, Jin X, Tang BT. A novel flexible phase change composite with electro-driven shape memory, energy conversion/storage and motion sensing properties. J Mater Chem A 2019;7(46):26385–92.
[11] Shuai C, Wang Z, Yang F, Zhang H, Liu J, Feng P. Laser additive manufacturing of shape memory biopolymer bone scaffold: 3D conductive network construction and electrically driven mechanism. J Adv Res 2023.
[12] Xie Y, Meng Y, Wang WX, Zhang E, Leng JS, Pei QB. Bistable and reconfigurable photonic crystals-electroactive shape memory polymer nanocomposite for ink-free rewritable paper. Adv Funct Mater 2018;28(34).
[13] Liang RX, Yu HJ, Wang L, Wang N, Amin BU. NIR light-triggered shape memory polymers based on mussel-inspired iron-catechol complexes. Adv Funct Mater 2021;31(32).
[14] Jin X, Liu X, Li XW, Du LP, Su L, Ma YL, et al. High lignin, light-driven shape memory polymers with excellent mechanical performance. Int J Biol Macromol 2022;219:44–52.
[15] Wang W, Shen DF, Li X, Yao Y, Lin JP, Wang A, et al. Light-driven shape-memory porous films with precisely controlled dimensions. Angewandte Chemie-Int Edition 2018;57(8):2139–43.
[16] Hanif M, Zhang L, Shah AH, Chen ZW. Mechanical analysis and biodegradation of oxides-based magneto-responsive shape memory polymers for material extrusion 3D printing of biomedical scaffolds. Addit Manuf 2024;86.
[17] Liu JAC, Gillen JH, Mishra SR, Evans BA, Tracy JB. Photothermally and magnetically controlled reconfiguration of polymer composites for soft robotics. Sci Adv 2019;5(8).
[18] Ha M, Bermúdez GSC, Liu JAC, Mata ESO, Evans BA, Tracy JB, et al. Reconfigurable magnetic origami actuators with on-board sensing for guided assembly. Adv Mater 2021;33(25).
[19] Han XJ, Dong ZQ, Fan MM, Liu Y, Li JH, Wang YF, et al. pH-induced shape-memory polymers. Macromol Rapid Commun 2012;33(12):1055–60.
[20] Zhou K, Sun RJ, Wojciechowski JP, Wang R, Yeow J, Zuo YY, et al. 4D multimaterial printing of soft actuators with spatial and temporal control. Adv Mater 2024;36(19).
[21] Sun JH, Peng B, Lu Y, Zhang X, Wei J, Zhu CY, et al. A photoorganizable triple shape memory polymer for deployable devices. Small 2022;18(9).
[22] Zhang B, Li HG, Cheng JX, Ye HT, Sakhaei AH, Yuan C, et al. Mechanically robust and UV-curable shape-memory polymers for digital light processing based 4D printing. Adv Mater 2021;33(27).
[23] Luo L, Zhang FH, Wang LL, Liu YJ, Leng JS. Multidimensional cross-linked network strategies for rapidly, reconfigurable, refoldable shape memory polymer. Chem Eng J 2023;478.
[24] Li YJ, Zhang FH, Liu YJ, Leng JS. A tailorable series of elastomeric-to-rigid, selfhealable, shape memory bismaleimide. Small 2023.
[25] Hu RX, Zhang FH, Luo L, Wang LL, Liu YJ, Leng JS. An end-capping strategy for shape memory phthalonitrile resins via annealing enables conductivity and wave-absorption. Chem Eng J 2024;489.
[26] Zhang F, Wang L, Geng Q, Liu Y, Leng J, Smoukov SKK. Adjustable volume and loading release of shape memory polymer microcapsules. Int J Smart and Nano Materials 2023;14(1):77–89.
[27] Wang L, Ma J, Guo T, Zhang F, Dong A, Zhang S, et al. Control of surface wrinkles on shape memory PLA/PPDO micro-nanofibers and their applications in drug release and anti-scarring. Adv Fiber Mater 2023;5(2):632–49.
[28] Lendlein A. Fabrication of reprogrammable shape-memory polymer actuators for robotics. Sci Rob 2018;3(18).
[29] Wang YC, Wang YZ, Shu JC, Cao WQ, Li CS, Cao MS. Graphene implanted shape memory polymers with dielectric gene dominated highly efficient microwave drive. Adv Funct Mater 2023;33(40).
[30] Curtis SM, Sielenkaemper M, Arivanandhan G, Dengiz D, Li Z, Jetter J, et al. TiNiHf/SiO2/Si shape memory film composites for bi-directional micro actuation. Int J Smart and Nano Materials 2022;13(2):293–314.
[31] Yan SY, Zhang FH, Luo L, Wang LL, Liu YJ, Leng JS. Shape memory polymer composites: 4D printing, smart structures, and applications. Research 2023;6.
[32] Luo L, Zhang FH, Wang LL, Liu YJ, Leng JS. Recent advances in shape memory polymers: multifunctional materials, multiscale structures, and applications. Adv Funct Mater 2024;34(14).
[33] Du HY, Liu LW, Leng JS, Peng HX, Scarpa F, Liu YJ. Shape memory polymer S-shaped mandrel for composite air duct manufacturing. Compos Struct 2015;133:930–8.
[34] Du HY, Liu LW, Zhang FH, Leng JS, Liu YJ. Shape retainability and reusability investigation of bottle-shaped SMP mandrel. Polym Test 2018;69:325–31.
[35] Zhang L, Du HY, Liu LW, Liu YJ, Leng JS. Analysis and design of smart mandrels using shape memory polymers. Composites Part B-Eng 2014;59:230–7.
[36] Everhart MC, Stahl J. Reusable shape memory polymer mandrels. Smart Structures and Materials 2005 Conference. San Diego, CA2005. p. 27-34.
[37] Zhang DW, Wang XG, Zhang WY, Liu YJ, Leng JS. Shape memory polymer networks from styrene copolymer. International Conference on Smart Materials and Nanotechnology in Engineering. Harbin Inst Technol, Harbin, PEOPLES R CHINA2007.
[38] Meiorin C, Mosiewicki MA, Aranguren MI. Ageing of thermosets based on tung oil/styrene/divinylbenzene. Polym Test 2013;32(2):249–55.
[39] Li HZ, Luo YW, Gao X. Preparation of soft shape memory polymer and its application as a compliant thermal-triggered gripper. Macromol Chem Phys 2019;220(15).
[40] Zeng YN, Yang WM, Liu SX, Shi XH, Xi AQ, Zhang FA. Dynamic semi IPNs with duple dynamic linkers: self-healing, reprocessing, welding, and shape memory behaviors. Polymers 2021;13(11).
[41] Li FK, Hasjim J, Larock RC. Synthesis, structure, and thermophysical and mechanical properties of new polymers prepared by the cationic copolymerization of corn oil, styrene, and divinylbenzene. J Appl Polym Sci 2003;90(7):1830–8.
[42] Li FK, Larock RC. Novel polymeric materials from biological oils. J Polym Environ 2002;10(1–2):59–67.
[43] Xie F, Huang CW, Wang F, Huang LN, Weiss RA, Leng JS, et al. Carboxyl-terminated polybutadiene poly(styrene-co-4-vinylpyridine) supramolecular thermoplastic elastomers and their shape memory behavior. Macromolecules 2016;49(19):7322–30.